frontiers in Materials

ORIGINAL RESEARCH
published: 11 March 2022
doi: 10.3389/fmats.2022.856000

Hall Effect Study of the Metamagnetic Transition in the $Sr_4(Ru_{0.99}Fe_{0.01})_3O_{10}$ Nanosheet

Jiajie Wan[1], Yan Liu[2], Yuanqing Wan[1], Qing Wu[1], Yu Wang[3], Jiyong Yang[1], Zhiqiang Mao[3] and Junzhong Wang[1]*

[1]School of Physical Science and Technology, Southwest University, Chongqing, China, [2]Analytical and Testing Center, Chongqing University, Chongqing, China, [3]Department of Physics, Pennsylvania State University, University Park, PA, United States

$Sr_4(Ru_{0.99}Fe_{0.01})_3O_{10}$ shows a ferromagnetic (FM) transition at $T_C \sim 105$ K with the magnetic easy axis in the *ab* plane, followed by a metamagnetic transition (MMT) at low temperatures when the magnetic field *H* is applied along the *c* axis, which is in sharp contrast to that of the pure $Sr_4Ru_3O_{10}$, where the easy axis is along the *c* axis and the MMT is in the *ab* plane. Here, we studied the MMT in the $Sr_4(Ru_{0.99}Fe_{0.01})_3O_{10}$ nanosheet by the Hall effect. It was found that the ordinary Hall coefficient of $Sr_4(Ru_{0.99}Fe_{0.01})_3O_{10}$ is almost the same as that of the pure $Sr_4Ru_3O_{10}$, while a sudden increase in the Hall resistance R_{xy} is observed below ~50 K, above which the R_{xy} presents the conventional anomalous Hall effect up to T_C. Analysis of the results indicates that the MMT has no direct correlation to the electronic structure but closely relates to the magnetic moment locking, where the magnetic-field-induced breakdown of the locked moments is responsible for the MMT.

Keywords: metamagnetic transition, Hall effect, $Sr_4(Ru_{0.99}Fe_{0.01})_3O_{10}$, magnetic moment locking, ferromagnetic transition

OPEN ACCESS

Edited by:
Xu Zuo,
Nankai University, China

Reviewed by:
Mingliang Tian,
Hefei Institutes of Physical Science (CAS), China
Liang Li,
Hefei Institutes of Physical Science (CAS), China

****Correspondence:***
Jiyong Yang
jyyang@swu.edu.cn

Specialty section:
This article was submitted to Quantum Materials, a section of the journal Frontiers in Materials

Received: *16 January 2022*
Accepted: *31 January 2022*
Published: *11 March 2022*

Citation:
Wan J, Liu Y, Wan Y, Wu Q, Wang Y, Yang J, Mao Z and Wang J (2022) Hall Effect Study of the Metamagnetic Transition in the $Sr_4(Ru_{0.99}Fe_{0.01})_3O_{10}$ Nanosheet. Front. Mater. 9:856000. doi: 10.3389/fmats.2022.856000

INTRODUCTION

The 4*d*-electron-based perovskite ruthenium oxides $Sr_{n+1}Ru_nO_{3n+1}$ (n = 1, 2, ∞) with a strong inherent spin orbital coupling present rich and fascinating phenomena, such as unconventional superconductivity (Sr_2RuO_4, n = 1) (Mackenzie and Maeno, 2003), magnetic-field-tuned metamagnetic quantum criticality ($Sr_3Ru_2O_7$, n = 2) (Grigera et al., 2001), and itinerant ferromagnetism ($SrRuO_3$, n = ∞) (Koster et al., 2012). In contrast, the n = 3 member $Sr_4Ru_3O_{10}$ is an exotic ferromagnetic (FM) metal (Crawford et al., 2002). It possesses an orthorhombic unit cell composed of triple layers of corner-shared RuO_6 octahedra separated by double rock-salt Sr-O layers. The RuO_6 octahedra in the outer two layers of each triple layer are rotated by an average of 5.25° around the *c*-axis, while the octahedra of the inner layers are rotated in the opposite sense by an average of 10.6° (Crawford et al., 2002). $Sr_4Ru_3O_{10}$ undergoes an FM transition at a Curie temperature $T_C \sim 105$ K with the easy axis along the *c* axis, followed by a second transition at a critical temperature $T_M \sim 50$ K (Crawford et al., 2002; Cao et al., 2003). Below T_M, a superlinear increase of magnetization, i.e., a metamagnetic transition (MMT), is observed when the magnetic field is applied in the *ab* plane (Cao et al., 2003).

The MMT in $Sr_4Ru_3O_{10}$ has been widely investigated, but its nature remains elusive (Lin et al., 2004; Gupta et al., 2006; Mao et al., 2006; Jo et al., 2007; Schottenhamel et al., 2016). The magnetization and Raman spectrum studies suggest that the MMT is associated with a magnetic-field-induced breakdown of the antiferromagnetic (AFM) order in the *ab* plane below

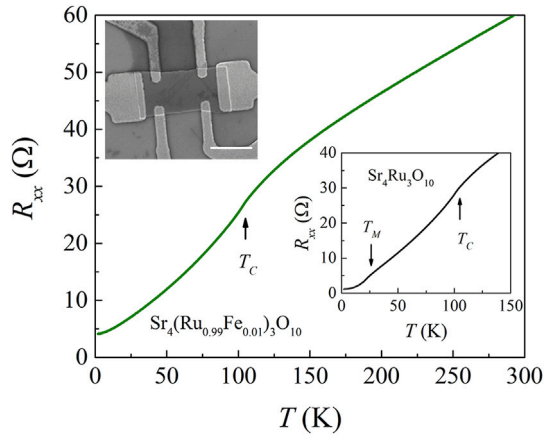

FIGURE 1 | The temperature dependence of the zero-field resistance R_{xx} of a 45-nm-thick $Sr_4(Ru_{0.99}Fe_{0.01})_3O_{10}$ nanosheet. Insets (top) SEM image of the $Sr_4(Ru_{0.99}Fe_{0.01})_3O_{10}$ nanosheet with electrodes, scale bar: 3 μm. (Bottom) R_{xx}–T curve of a pure $Sr_4Ru_3O_{10}$ nanosheet with the thickness of about 35 nm.

T_M through a spin-flip process (Cao et al., 2003; Gupta et al., 2006). However, no AFM order in the *ab* plane is detected by neutron diffraction measurements (Granata et al., 2013; Zhu et al., 2018). On the other hand, systematical transport studies on the $Sr_4Ru_3O_{10}$ nanosheets show that the MMT is likely an in-plane magnetic-field-induced spin-flop process from the *c* axis to the *ab* plane (Liu et al., 2018).

Interestingly, when the Ru is substituted by a small amount of Fe [$Sr_4(Ru_{0.99}Fe_{0.01})_3O_{10}$], the magnetic behavior is changed significantly (Liu et al., 2019). It is found that the magnetic easy direction is fully changed from the *c* axis to the *ab* plane below T_C and that the second transition at T_M, which usually occurs in pure $Sr_4Ru_3O_{10}$ crystals, is not seen though the FM transition remains at 105 K. In addition, an MMT is observed when the magnetic field is applied along the *c* direction. The Fe doping opens a path to explore the nature of the MMT by using $Sr_4(Ru_{0.99}Fe_{0.01})_3O_{10}$ as a model system. Here, we perform a systematical Hall effect measurement of the MMT in the $Sr_4(Ru_{0.99}Fe_{0.01})_3O_{10}$ nanosheet, which contains both the ordinary Hall effect and the anomalous Hall effect. Results show that the MMT has less correlation to the electronic structure but depends on the magnetic moment locking.

MATERIALS AND METHODS

The $Sr_4(Ru_{0.99}Fe_{0.01})_3O_{10}$ single crystals were grown by the floating zone method as described in Liu et al. (2019). The starting materials were $SrCO_3$, Fe_2O_3, and RuO_2. Twenty-five percent excess RuO_2 was added to compensate the evaporation of RuO_2 from the melting zone. The mixed powder was ground for ~1 h, and then pressed into pellets, after which, the pellets were sintered at a temperature of about 900°C for 12 h. The sintered pellets were ground for ~1 h again, and the ground powder was pressed to a rod and sintered at a temperature of 1,350°C for 4 h. The pressure in the quartz tube was ~10 bar (10% O_2 + 90% Ar), and the growth speed was about ~15 mm/h.

The concentration of Fe was analyzed roughly by energy-dispersive spectrum (EDS, Oxford Instruments). $Sr_4(Ru_{0.99}Fe_{0.01})_3O_{10}$ nanosheets were obtained by the scotch tape-based micro-mechanical exfoliation method from the bulk single crystal and then transferred onto a SiO_2 (300 nm)/Si substrate. Contacts were patterned using the electron-beam lithography technique followed by deposition of Ti/Au (5/100 nm). The scanning electron microscope (SEM) image of a device with patterned electrodes is shown in the top inset of **Figure 1**. The thickness of the nanosheet is about 45 nm, which is determined by the atomic force microscopy. The transport property of the nanosheet was measured by a physical property measurement system (PPMS, Quantum Design). The Hall resistance R_{xy} is determined from $R_{xy} = [R_{xy}(H) - R_{xy}(-H)]/2$ in order to subtract the component of the longitudinal resistance R_{xx} arising from the small misalignment of transverse contacts.

RESULTS AND DISCUSSION

Figure 1 shows the temperature T-dependent longitudinal resistance R_{xx} of the $Sr_4(Ru_{0.99}Fe_{0.01})_3O_{10}$ nanosheet, which is measured at zero magnetic field. It is found that the R_{xx} decreases monotonously as the temperature decreases, indicating a metallic behavior of the nanosheet. An anomaly of the resistance near T_C ~ 105 K can be identified due to the FM transition, but no second anomaly at T_M is seen, which is in sharp contrast to that observed in the pure $Sr_4Ru_3O_{10}$ bulk or nanosheets, where two resistive anomalies at T_C and T_M can be found (Liu et al., 2018; Liu et al., 2017). For a comparison, the R_{xx}–T property of a pure $Sr_4Ru_3O_{10}$ nanosheet with thickness of about 35 nm is presented in the bottom inset of **Figure 1**. Note that the T_M of the pure nanosheet

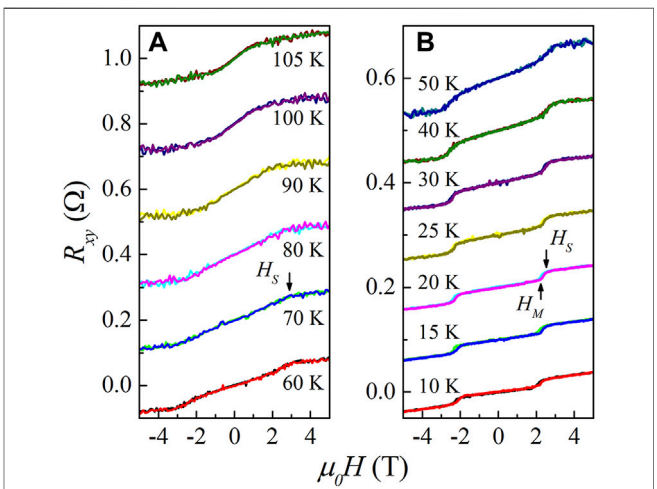

FIGURE 2 | (A) and **(B)** Hall resistance R_{xy} of the 45-nm-thick $Sr_4(Ru_{0.99}Fe_{0.01})_3O_{10}$ nanosheet as a function of perpendicular magnetic field H at various temperatures. Data have been shifted vertically for clarity.

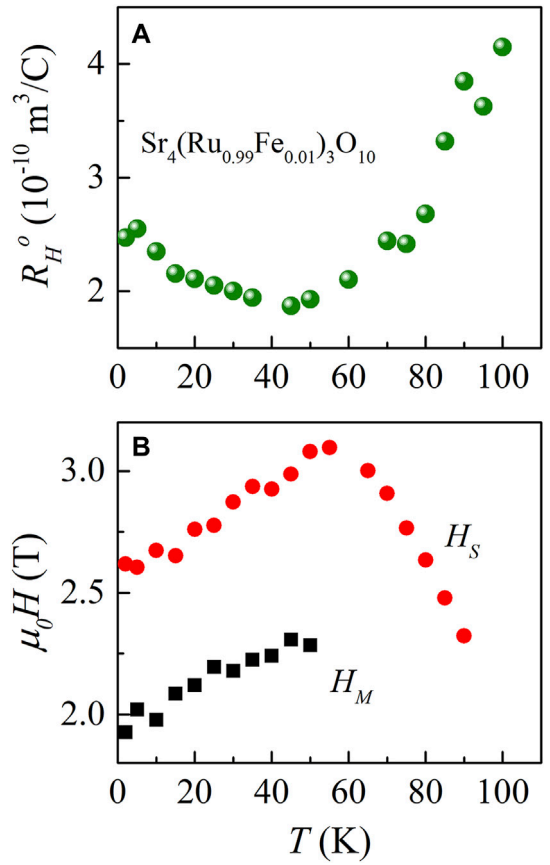

FIGURE 3 | (A) The ordinary Hall coefficient R_H^o of the $Sr_4(Ru_{0.99}Fe_{0.01})_3O_{10}$ nanosheet as a function of temperature. **(B)** Temperature-dependent critical field H_M of the MMT and the saturation field H_S.

is about 25 K, which is smaller than that of the pure bulk due to the size effect (Liu et al., 2016).

Figure 2 shows the magnetic field H-dependent Hall resistance R_{xy} of the $Sr_4(Ru_{0.99}Fe_{0.01})_3O_{10}$ nanosheet measured at various temperatures, where H is applied perpendicular to the ab plane of the nanosheet. It is found that all the R_{xy}–H curves below $T_C \sim 105$ K can be well described by Nagaosa et al. (2010)

$$R_{xy} = R_{xy}^o + R_{xy}^a \quad (1)$$

The R_{xy}^o is the ordinary Hall resistance determined by the electronic structure and can be written as $R_{xy}^o = R_H^o H/t$, with R_H^o and t being the ordinary Hall coefficient and the thickness of the sample, respectively; R_{xy}^a is the anomalous Hall resistance, which is proportional to the magnetization M_c along the c axis, i.e., $R_{xy}^a = R_H^a M_c/t$, with R_H^a being the anomalous Hall coefficient. Therefore, the Hall effect measurement is a powerful tool to measure both the electronic structure and the magnetization M_c of the $Sr_4(Ru_{0.99}Fe_{0.01})_3O_{10}$ nanosheet. It is seen that

(1) The R_{xy} increases almost linearly as H increases in the temperature range of $T^* \sim 50$ K $< T < T_C$ (**Figure 2A**) and then turns to saturation at a magnetic field H_S. This anomalous Hall effect is very similar to that observed in many other FM materials (Nagaosa et al., 2010). Since the magnetic easy axis of $Sr_4(Ru_{0.99}Fe_{0.01})_3O_{10}$ is in the ab plane, this behavior indicates that the magnetic moments at $T^* < T < T_C$ are rotated collectively from the ab plane to the c axis by H.

(2) At $T < T^*$, the R_{xy} first increases linearly as the magnetic field increases and then followed by a sharp increase at a magnetic field H_M, which is slightly below the saturation field H_S as indicated in **Figure 2B**. Above H_S, the R_{xy} increases linearly. According to **Eq. 1**, this behavior demonstrates that there is a rapid increase of M_c at $H_M < H < H_S$, i.e., an MMT in the $Sr_4(Ru_{0.99}Fe_{0.01})_3O_{10}$ nanosheet as the sweeping of H along the c direction, which is in contrast to that of the pure $Sr_4Ru_3O_{10}$, where the MMT is in the ab plane (Cao et al., 2003). The H_M can thus be defined as the critical field of the MMT.

To better understand the MMT, we firstly focus on the ordinary Hall effect of the $Sr_4(Ru_{0.99}Fe_{0.01})_3O_{10}$ nanosheet. **Figure 3A** shows the ordinary Hall coefficient R_H^o as a function of temperature, which is extracted from the high field slope of the Hall isotherm at $H = 5$ T ($>H_S$). The R_H^o is positive in the whole temperature range, indicating that the dominant carriers in the $Sr_4(Ru_{0.99}Fe_{0.01})_3O_{10}$ nanosheet are holes. Except for the R_H^o of the $Sr_4(Ru_{0.99}Fe_{0.01})_3O_{10}$ nanosheet at low temperatures being slightly smaller, the trace of the R_H^o–T curve here is very similar to that reported in the pure $Sr_4Ru_3O_{10}$ nanosheet (Liu et al., 2016). Considering that the FM moment in $Sr_4(Ru_{0.99}Fe_{0.01})_3O_{10}$ is in the ab plane and the MMT is along the c direction, which is completely different to that in the pure $Sr_4Ru_3O_{10}$, where the FM moment is along the c direction and the MMT is in the ab plane, the almost identical R_H^o indicates that the MMT has no direct correlation to the electronic structure, but only the spin-flop from the ab plane to the c direction.

To give an insight of the MMT, we reinspect the Hall data shown in **Figure 2**. One can see that at 10 K, the slope of the R_{xy}–H curve below H_M is almost the same as that at $H > H_S$. The change of R_{xy} above H_S is purely due to the orbital effect of H on carriers, i.e., the ordinary Hall resistance R_{xy}^o, while that below H_M is the sum of both the change of R_{xy}^o and R_{xy}^a. The almost identical slope of the R_{xy}–H curve at $H < H_M$ and $H > H_S$ indicates that the R_{xy}^a is about zero (where $M_c = 0$) at $H < H_M$. In other words, the magnetic moments are fully "locked" without any net moment along the c direction below H_M. As the T increases, the slope of the R_{xy}–H curve at $H < H_M$ becomes larger than that at $H > H_S$, indicating that some magnetic moments are unlocked due to the thermal activation. At $T > T^* \sim 50$ K, all the magnetic moments become a collective rotation under the magnetic field as mentioned above; hence, the MMT vanishes. This result indicates that the spin-flop is associated with a magnetic-field-induced breakdown of the locking moments, which is responsible for the MMT.

An unexpected feature seen in **Figure 2** is that both H_M and H_S decrease with decreasing T below T^*, which means intuitively that it is easier to align the magnetic moments along the c direction with decreasing temperature by the magnetic field. To see clearly, the temperature dependence of H_M and H_S is shown in **Figure 3B**. This behavior is in contrast to that of conventional magnetic materials, in which the magnetic moments are usually difficult to

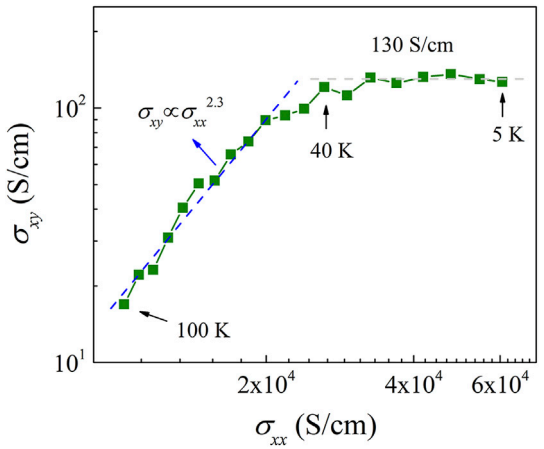

FIGURE 4 | The scaling relation between the anomalous Hall conductivity σ_{xy} and the longitudinal conductivity σ_{xx}.

polarize to the magnetic hard axis at lower temperatures due to the reduction of thermal fluctuation.

We noticed that the *T*-dependent feature of the lattice parameter *c* of the pure $Sr_4Ru_3O_{10}$ shows a minimum at T^* (Granata et al., 2013; Schottenhamel et al., 2016), indicating a slightly negative expansion below T^*. This negative expansion nicely echoes the anomaly in H_M and R_H^o. As known previously (Liu et al., 2017; Liu et al., 2018), the shrinkage of the *c* axis will reduce the magnetocrystalline anisotropy energy and favors the magnetic moment off the *c* axis, such as the Fe-doping effect (Liu et al., 2019). The tiny expansion of the *c* axis below T^* will favor the FM moment off the *ab* plane, resulting in the decrease of the pinning force for moment locking in the *ab* plane. The critical magnetic field H_M is actually the competition between the moment locking force below T^* and the *c* axis expansion-induced depinning effect. This is the reason that the H_M decreases with decreasing *T*.

Finally, as a metamagnetic metal of $Sr_4(Ru_{0.99}Fe_{0.01})_3O_{10}$, we would like to present the scaling relation between the anomalous Hall conductivity σ_{xy} and the longitudinal conductivity σ_{xx} of $\sigma_{xy} \propto \sigma_{xx}^{\varphi}$, where φ is the scaling exponent, which is shown in **Figure 4**. The σ_{xy} is determined by $\sigma_{xy} = \rho_{xy}^a/[(\rho_{xx})^2 + (\rho_{xy}^a)^2]$ with ρ_{xx} being the longitudinal resistivity and ρ_{xy}^a the anomalous Hall resistivity at zero field, which is obtained by extrapolating the high-field linear term of the Hall data to the zero field shown in **Figure 2**. It is found that at $T > 60$ K, $\varphi = 2.3$, indicating that the side jump mechanism is dominant (Nagaosa et al., 2010). Below 40 K, $\varphi = 0$ with $\sigma_{xy} = 130$ S/cm, which can be attributed to the intrinsic dissipationless topological Berry-phase contribution (Nagaosa et al., 2010). The scaling relation is almost the same as many conventional FM materials (Nagaosa et al., 2010), indicating a regular FM nature of $Sr_4(Ru_{0.99}Fe_{0.01})_3O_{10}$ after being polarized.

CONCLUSION

We have investigated the MMT of $Sr_4(Ru_{0.99}Fe_{0.01})_3O_{10}$ along the *c* axis by Hall effect. Results show that the ordinary Hall coefficient is almost the same as that of the pure $Sr_4Ru_3O_{10}$. The magnetic moments are found to be fully locked without any net moments along the *c* direction at the ground state at 10 K and then gradually unlocked with increasing *T*. At about 50 K, the magnetic moments are fully depinned, and the MMT smears out. Our result indicates that the MMT has less correlation to the electronic structure but closely relates to the magnetic moment locking.

DATA AVAILABILITY STATEMENT

The original contributions presented in the study are included in the article/Supplementary Material, further inquiries can be directed to the corresponding author.

AUTHOR CONTRIBUTIONS

JW, YL, YW, and QW carried out the experiments of EBL and transport measurement. YW and ZM synthesized the sample. JW, JY, and JW wrote and reviewed the manuscript with the help of all authors.

FUNDING

This work was supported by the Fundamental Research Funds for the Central Universities (grant no. SWU019010), the Chongqing Municipal Program of Innovation and Entrepreneurship for Undergraduates (grant no. S202010635003), and the National Natural Science Foundation of China (grants nos. 11674323, 11804297, and U19A2093). The single-crystal growth effort was supported by the U.S. Department of Energy under EPSCoR Grant No. DE-SC0012432 with additional support from the Louisiana Board of Reagents.

REFERENCES

Cao, G., Balicas, L., Song, W. H., Sun, Y. P., Xin, Y., Bondarenko, V. A., et al. (2003). Competing Ground States in Triple-layeredSr4Ru3O10:Verging on Itinerant Ferromagnetism with Critical Fluctuations. *Phys. Rev. B* 68, 174409. doi:10.1103/physrevb.68.174409

Crawford, M. K., Harlow, R. L., Marshall, W., Li, Z., Cao, G., Lindstrom, R. L., et al. (2002). Structure and Magnetism of Single crystalSr4Ru3O10: A Ferromagnetic Triple-Layer Ruthenate. *Phys. Rev. B* 65, 214412. doi:10.1103/physrevb.65.214412

Granata, V., Capogna, L., Reehuis, M., Fittipaldi, R., Ouladdiaf, B., Pace, S., et al. (2013). Neutron Diffraction Study of Triple-Layered Sr4Ru3O10. *J. Phys. Condens. Matter* 25, 056004. doi:10.1088/0953-8984/25/5/056004

Grigera, S. A., Perry, R. S., Schofield, A. J., Chiao, M., Julian, S. R., Lonzarich, G. G., et al. (2001). Magnetic Field-Tuned Quantum Criticality in the Metallic Ruthenate Sr 3 Ru 2 O 7. *Science* 294, 329–332. doi:10.1126/science.1063539

Gupta, R., Kim, M., Barath, H., Cooper, S. L., and Cao, G. (2006). Field- and Pressure-Induced Phases in $Sr_4Ru_3O_{10}$: a Spectroscopic Investigation. *Phys. Rev. Lett.* 96, 067004. doi:10.1103/physrevlett.96.067004

Jo, Y. J., Balicas, L., Kikugawa, N., Choi, E. S., Storr, K., Zhou, M., et al. (2007). Orbital-dependent Metamagnetic Response in $Sr_4Ru_3O_{10}$. *Phys. Rev. B* 75, 094413. doi:10.1103/physrevb.75.094413

Koster, G., Klein, L., Siemons, W., Rijnders, G., Dodge, J. S., Eom, C.-B., et al. (2012). Structure, Physical Properties, and Applications ofSrRuO3thin Films. *Rev. Mod. Phys.* 84, 253–298. doi:10.1103/revmodphys.84.253

Lin, X. N., Bondarenko, V. A., Cao, G., and Brill, J. W. (2004). Specific Heat of Sr4Ru3O10. *Solid State. Commun.* 130, 151–154. doi:10.1016/j.ssc.2004.02.009

Liu, Y., Chu, W., Wang, Y., Yang, J., Du, H., Ning, W., et al. (2019). Fe-doping Induced Suppression of the Second Magnetic Transition in Sr4Ru3O10. *Phys. Rev. B* 99, 214418. doi:10.1103/physrevb.99.214418

Liu, Y., Chu, W. W., Yang, J. Y., Liu, G. Q., Du, H. F., Ning, W., et al. (2018). Magnetic Reversal in $Sr_4Ru_3O_{10}$ Nanosheets Probed by Anisotropic Magnetoresistance. *Phys. Rev. B* 98, 024425. doi:10.1103/physrevb.98.024425

Liu, Y., Yang, J., Wang, W., Du, H., Ning, W., Ling, L., et al. (2017). Evidence of In-Plane Ferromagnetic Order Probed by Planar Hall Effect in the Geometry-Confined Ruthenate Sr4Ru3O10. *Phys. Rev. B* 95 (R), 161103. doi:10.1103/physrevb.95.161103

Liu, Y., Yang, J., Wang, W., Du, H., Ning, W., Ling, L., et al. (2016). Size Effect on the Magnetic Phase in Sr4Ru3O10. *New J. Phys.* 18, 053019. doi:10.1088/1367-2630/18/5/053019

Mackenzie, A. P., and Maeno, Y. (2003). The Superconductivity ofSr2RuO4and the Physics of Spin-Triplet Pairing. *Rev. Mod. Phys.* 75, 657–712. doi:10.1103/revmodphys.75.657

Mao, Z. Q., Zhou, M., Hooper, J., Golub, V., and O'Connor, C. J. (2006). Phase Separation in the Itinerant Metamagnetic Transition of $Sr_4Ru_3O_{10}$. *Phys. Rev. Lett.* 96, 077205. doi:10.1103/physrevlett.96.077205

Nagaosa, N., Sinova, J., Onoda, S., MacDonald, A. H., and Ong, N. P. (2010). Anomalous Hall Effect. *Rev. Mod. Phys.* 82, 1539–1592. doi:10.1103/revmodphys.82.1539

Schottenhamel, W., Abdel-Hafiez, M., Fittipaldi, R., Granata, V., Vecchione, A., Hücker, M., et al. (2016). Dilatometric Study of the Metamagnetic and Ferromagnetic Phases in the Triple-Layered Sr4Ru3O10 System. *Phys. Rev. B* 94, 155154. doi:10.1103/physrevb.94.155154

Zhu, M., Li, P. G., Wang, Y., Cao, H. B., Tian, W., Zhang, H. D., et al. (2018). Temperature- and Field-Driven Spin Reorientations in Triple-Layer Ruthenate Sr4Ru3O10. *Sci. Rep.* 8, 3914. doi:10.1038/s41598-018-22247-3

Conflict of Interest: The authors declare that the research was conducted in the absence of any commercial or financial relationships that could be construed as a potential conflict of interest.

Publisher's Note: All claims expressed in this article are solely those of the authors and do not necessarily represent those of their affiliated organizations, or those of the publisher, the editors and the reviewers. Any product that may be evaluated in this article, or claim that may be made by its manufacturer, is not guaranteed or endorsed by the publisher.